High resolution observations of the thermal tSZ effect from galaxy clusters

NIKA2 Guaranteed Time Large Program
300 h of allocated time

J. F. Macías-Pérez (LPSC), E. Pointecouteau (IRAP), B. Comis (LPSC), R. Adam (LPSC), N. Aghanim (IAS), M. Arnaud (CEA), F.X. Désert (IPAG), M. Douspis (IAS), F. Mayet (LPSC), J. B. Melin (CEA), L. Perotto (LPSC), G. Pratt (CEA), J. A. Rubiño-Martín (IAC), F. Ruppin (LPSC)

Abstract – We describe here the NIKA2 Guaranteed Time Large Program dedicated to high resolution observations of clusters of galaxies at intermediate and high redshift via the thermal Sunyaev-Zeldovich (tSZ) effect, for a total of 300 hours. We intend to observe a large sample of clusters (50 objects in total) representative of the cluster population in the redshift range from 0.5 to 1.5, for which the FOV and resolution of NIKA2 are particularly well adapted. The main output of the program will be: i) the study of the redshift evolution of the cluster pressure profile and of the scaling laws relating cluster observational properties (i.e. the integrated Compton parameter and the cluster total masses), ii) the study of the dispersion of the cluster population around its average behaviour and its correlation with the morphology and dynamical state of the objects (at z > 0.5). This will be achieved through NIKA2 sub-arcminute resolution tSZ observations, leading to major improvements on the use of clusters of galaxies to draw cosmological constraints.

Scientific context – As the largest gravitationally collapsed objects in the universe, clusters of galaxies represent the last step of the hierarchical gravitational process of structure formation. Therefore their abundance in mass and redshift is strongly related to the power spectrum of the primordial density fluctuations, to the cosmological parameters and their evolution all along the history of our Universe.

Most of the cluster baryons are present as a diffuse gas, the Intra-Cluster Medium (ICM), hot (10^6 - 10^8 K) and completely ionized. Due to its physical state, the ICM is responsible for a secondary anisotropy of the Cosmic Microwave Background (CMB): the thermal Sunyaev-Zel'dovich (tSZ) effect. Through their path toward us, CMB photons may interact with the free hot electrons in the ICM, being then shifter to higher energies. This results in a CMB flux decrement (increment) at frequencies below (above) 217 GHz, which corresponds to a distortion of the CMB spectrum. The amplitude of the effect is proportional to the integral of the pressure of the electron population along the line of sight ($y \propto \int P_e dl$). Measuring the distribution of the tSZ signal in clusters directly probes the distribution of thermal pressure within the ICM. Furthermore, being a CMB spectral distortion, the tSZ flux is not affected by redshift cosmic dilution. Thus, the tSZ effect represents an interesting observable to detect and study clusters at high redshifts, where their number and distribution is the most sensitive to the underlying cosmology (e.g. Carlstrom et al. 2002).

In the last few years, technological progresses have made possible to detect the tSZ effect routinely. As a consequence, tSZ-selected cluster catalogues containing several thousands of candidates have finally been produced, at arcmin resolution, by the South Pole Telescope (SPT, FWHM ∼ 1.1 arcmin at 150 GHz, Reichardt et al. 2013; Bleem et al. 2014), the Atacama Cosmology Telescope (ACT, FWHM ∼ 1.4 arcmin at 148 GHz, Hasselfield et al. 2013), the Planck satellite (FWHM ∼ 10 arcmin for tSZ, Planck Collaboration et al. 2014, 2015a). ICM observables, such as the tSZ flux, can provide a valuable tool for cosmological investigation with clusters, as long as we are able to convert them into robust mass estimates. In fact, at present, the systematic uncertainties affecting the observable to mass relations represent the limit for cluster-derived cosmological constraints. Planck, ACT and SPT have detected many clusters through tSZ performing a blind survey able to use this effect to identify objects not yet discovered at other wavelengths. However, their relatively limited resolution ($\gtrsim$ 1 arcmin) only allows detailed study of the spatial distribution of the signal for low redshift clusters. However, the use of tSZ-selected cluster samples for cosmological purposes also requires an accurate understanding of the astrophysical systematics affecting the baryonic proxies (i.e. the tSZ integrated flux, Y) of the cluster total mass (M_{tot}), even at high-z. In this context, **measurements reaching sub-arcminute angular resolution for cluster pressure profiles are a mandatory step for precise cluster and tSZ cosmology, since they will contribute to improve our knowledge of the statistical properties of galaxy cluster structure reducing the related uncertainties and biases, which now limit cosmological studies** (e.g. Planck Collaboration et al. 2015b,c).

Such measurements can only be made possible by high sensitivity and high spatial resolution tSZ observations. The NIKA2 camera at the IRAM 30 m telescope is a well-suited instrument for this kind of observations and follow-ups, given its resolution, sensitivity and dual-band observation capability (as it will be detailed later). Conducting

sub-arcminute tSZ observations of a representative population of clusters across a large redshift range will bring detailed insight of the properties of clusters over more than 3 Gyr. This will allow us to understand the processes driving the physical evolution of massive halos in the universe and to quantify how the cluster thermal content and distribution evolves as massive halos continue to grow through accretion and merging processes.

Objectives and main foreseen outpus –

The main objective of this program is to obtain **high resolution** tSZ observations for a sample of objects, which are **representative** of the population of clusters of galaxies, at **intermediate and high redshifts (z > 0.5)** and spanning more that an order of magnitude in Y_{500} (and then also in M_{500}). These observations will be used for an in-depth study the evolution of cluster physical properties across cosmic times. At present, cluster and tSZ derived cosmological constraints are limited by our incomplete understanding of the impact of the details of cluster astrophysics. Thus, this study is mandatory to handle systematics and achieve precision cosmology with clusters. More precisely we aim at:

- Exploring and test the regularity of the cluster pressure profile at z > 0.5, reproducing what has been done with the REXCESS sample at z < 0.2 (Arnaud et al. 2010), but with an observable (the SZ signal) that probes directly the ICM pressure. Is still pressure the quantity less affected by the cluster dynamical state and thermodynamic history, event high-z?

- Detecting the presence of sub-structures (e.g. secondary peaks, deviations from spherical symmetry, overall irregular shape) and their significance.

- Introduce, define and test parameters that allow us to quantify the cluster dynamical state through its tSZ morphology. A robust tSZ-defined indicator of cluster morphology would permit to study the disturbed cluster fraction as a function of redshift and would represent a useful tool to explore its correlation with deviation from the self-similar behavior (for both the pressure profile and scaling laws).

- Study the correlation between the SZ indicator(s) of cluster dynamical state and the dispersion around the average cluster pressure profile. Does the dispersion increase with redshift? Is it the same at any radial scale?

Target selection–

Our target selection strategy is mainly driven by the need of selecting **a sample of objects which is representative of the cluster population**. A flux selected subset of an tSZ-selected catalogue can be considered as representative of a sample that is not biased towards a given morphology. **We want to derive relations that can be applicable to the whole cluster population** (not only relaxed or un-relaxed) **in order to achieve a good global characterization of clusters and an improved control of systematics due to their astrophysics**. This criterion follows in fact the approach adopted to build the REXCESS sample (Böhringer et al. 2007), an XMM-Newton large program dedicated to the in-depth study of a representative sample of 33 clusters (0.055 < z < 0.183). This sample has in fact been used to build the universal pressure profile for the ICM (Arnaud et al. 2010, an average profile for the cluster population, derived from observations, scaled by mass and redshift according to the standard self-similar model).

In order to fulfill our goal with NIKA2, we consider the following main target selection criteria:

- clusters belonging to tSZ selected samples (already existing tSZ based cluster samples from Planck and ACT), for which the redshift information is available;

- z > 0.5, going up to to 1.5, to explore the cluster statistical properties beyond the local Universe;

- dec > -11, to ensure observability of the sources from the Pico Veleta site.

The number of objects fulfilling these requirement are provided in Tab. 1. The right panel of Fig. 1 shows those objects in the z - Y_{500} plane.

Sub-arcminute resolution tSZ observations with NIKA2 – The NIKA2 camera is particularly well adapted for high resolution observations of the tSZ effect from cluster of galaxies:

a) It operates simultaneously at two frequency bands, 150 and 260 GHz, at which tSZ shows up as a negative and a positive distortion of the CMB spectrum, producing a very distinctive cluster signal on the observed maps. Dual-band observations can be used to remove the atmospheric noise without affecting the signal,

	0.5 ≤ z < 0.7	0.7 ≤ z < 0.9	0.9 ≤ z < 1.1	no z available
PSZ1	40	11	-	153
PSZ2	21	2	-	150
ACT	19	11	2	

Table 1: Number of clusters extracted from the Planck (PSZ1 and PSZ2) and ACT (equatorial) tSZ-selected samples (Fig. 2). One of the ACT clusters (in the 0.7 ≤ z < 0.9 redshift interval) belongs also to the PSZ1 catalog. The table shows the number of objects, per bin in redshift, that are observables from the Pico Veleta site (dec > -11). For PSZ2 we only consider clusters that were not already present within PSZ1, that are not flagged as potential IR sources and for which $Q_{neural} > 0.4$ (Planck Collaboration et al. 2015a; Aghanim et al. 2014).

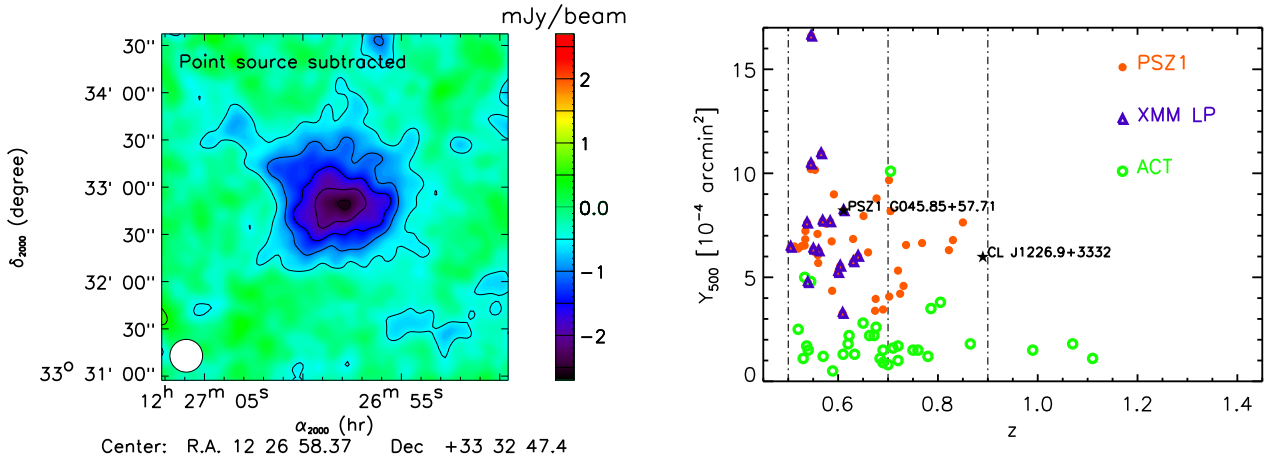

Figure 1: **Left:** NIKA map of CL J1226.9+3332 at 150 GHz (from Adam et al. 2015). The effective beam FWHM (18.2 arcsec native resolution plus an extra 10 arcsec FWHM Gaussian) is shown as the bottom left white circle. The overall effective observing time on the cluster is 7.8 hours and $\theta_{500} \sim 2$ arcmin for this cluster. **Right:** Clusters extracted from the Planck and ACT (equatorial) tSZ-selected samples, in the redshift range we want to explore and observables from the Pico Veleta site (dec > -11). As a function of redshift, we show the integrated tSZ signal (left) and the tSZ-estimated cluster total (right) mass of the sample of objects fulfilling our redshift (> 0.5) and observability (dec > -11) criteria. As a reference we show the high redshift cluster CL J1226.9+3332 and the Planck discovered PSZ1 G045.85+57.71, that have both been successfully observed by NIKA. The blue triangles represent the objects that have been already selected also for an on-going XMM large program (P.I.: M. Arnaud).

taking advantage of the characteristic tSZ spectrum (and then recover both small and large angular scales with the price of a worse sensitivity). In addition they are of the outmost interest to detect foreground contaminating sources, and account for their flux.

b) NIKA2 is made of arrays of thousands of high sensitive Kinetic Inductance Detectors (KIDs). In particular we expect a sensitivity in Compton parameter units of $\sim 10^{-4}$ per hour and per beam. This should allow us to obtain reliable tSZ detections and mapping of clusters of galaxies in few hours.

c) NIKA2, coupled to the IRAM 30 m telescope allows us to map clusters of galaxies to a resolution of typically 20 arcsec within a 6.5 arcmin diameter FOV. This is well adapted for medium and high redshift clusters for which we expect typical angular sizes of about 6-11 arcmin.

NIKA2 tSZ capabilities have been demonstrated through a pilot study conducted with its pathfinder, NIKA. In the context of this pilot study, in order to validate the KIDs capabilities when dealing with such a faint and diffuse signal, we have mapped the tSZ signal in the direction of six clusters of galaxies: **i)** RX J1347.5-1145, an intermediate redshift object (z=0.45), which is the perfect test target for the first tSZ detection ever achieved with KIDs (Adam et al. 2014b); **ii)** CL J1226.9+3332, a very high redshift cluster (z = 0.89, Adam et al. 2015, the tSZ map at 150 GHz is shown in the left panel of Fig. 1), **iii)** MACS J0717.5+3745, characterized by a complex morphology (Adam et al. 2014a); **iv)** MACS J1423.9+2404 a relaxed cluster, which was used to explore the impact of the presence of foreground radio and IR sources and how to deal with them in the data reduction (Adam et al. in prep.); **v)** PSZ1 G046.13+30.75 and PSZ1 G045.85+57.71, two newly Planck tSZ discovered clusters (at z=0.57 and z=0.61, respectively) chosen to test NIKA2 capabilities at the level of detection of the Planck catalogue of tSZ sources (NIKA Collaboration in prep.). We have successfully explored a wide range of cluster morphologies and amplitudes of the tSZ flux.
To date, the Mustang and Bolocam instruments (at the focus of the Green Bank Telescope and of the Caltech Submillimeter Observatory, respectively) have produced scientific quality tSZ observations (Korngut et al. 2011; Mroczkowski et al. 2012; Young et al. 2014; Sayers et al. 2011, 2013; Czakon et al. 2014). They are expected to be followed by next generation instruments, Mustang-2 and BolocamII, which represent the closest NIKA2 concurrent experiences. However, none of them will be operational before NIKA2 and none of them will combine sufficiently large FOV and high angular resolution to attempt the project described here. As an alternative to large diameter telescopes, interferometers (e.g. CARMA) can reach very high angular resolution, but they cannot recover the large scale signal and they are time expensive.

Observing strategy and data reduction – Based on the experience with the NIKA camera, we will perform OnTheFly (OTF) scans in right ascension and declination. We will alternate different orientations of the scans (e.g. 0, 45, 90,-45 degrees) and perform scans of 13' × 8' (about one third of the observing time will be spent on the core of the signal) so that we reach cluster outskirts (roughly up to twice the characteristic radius of the cluster r_{500}) even for the lowest redshift clusters. This will allow us to properly define the zero level of the final map and measure angular scales structures up to the scan size. Smaller scans of 11' × 7' will be considered in the case of high redshift and low mass clusters ($\theta_{500} < 2.25$ arcmin).

We take the Y_{500} ($Y_{500} = \int_{\Omega_{r_{500}}} y d\Omega$), M_{500} and redshift from the latest updated version of PSZ1 and the ACT catalogs. We then consider an universal pressure profile (Arnaud et al. 2010) to model the distribution of the signal around the cluster center for each given Y_{500}. The estimates of the required observation time are optimized cluster by cluster, in order to obtain an homogeneous sample in terms of signal to noise at a given characteristic radius (r_{500}). r_{500} is computed from the redshift and the tSZ-derived M_{500} reported in the catalogues, in order to have a homogeneous definition that only depends on the tSZ flux and the cluster distance.

To estimate the observing time needed per cluster we have performed simulations including signal, as just discussed, and noise. In terms of noise we have considered simulations taking the NIKA2 specification sensitivity at 2 mm of 20 mJy/beam/$s^{1/2}$, and increased the noise by 30 % to account for correlated noise extra variance. In addition, we have considered the real FOV of the instrument (6.5') and a FWHM of 20" at 2 mm. By contrast we have considered no atmospheric contamination and uniform weather conditions across the sample.

As one of the major objectifs of the project is to have a clear picture of the morphology of the clusters we need to set strong requirements on the signal-to-noise at the map level to ensure structures are significantly detected at least up to θ_{500}. As we expect the SZ signal to peak towards the center of the cluster this criteria also ensure significant detection in the inner part of the cluster. Assuming a perfect reconstruction of the cluster up to θ_{500} (no filtering) and requiring 4 σ detection at θ_{500} on the map for pixels of the size of the beam, we can compute the needed observing

time per cluster. In addition we also impose a minimum of 1 hour of integration per cluster to ensure sufficient scan redundancy. If the final instrument performance are improved with respect to the specifications we plan to keep the same number of clusters as well as of the same observation time per cluster in order to recover large scale structures beyond θ_{500}.

In terms of data reduction we will use the tSZ dedicated pipeline developed for the NIKA experiments. Needed improvements and updates will be directly carried out by our team.

List of targets – The current status of the follow-up observations of tSZ discovered Planck clusters (not fully completed) does not allow us to present a definitive catalogue of clusters of galaxies. However, using the above criteria and the Planck and ACT samples we have pre-selected a first sample of clusters of galaxies suitable for our purposes. From the total sample we have performed a selection assuming **two bins in redshift ($0.5 < z \leq 0.7$ and $0.7 < z \leq 0.9$)**. For each interval in redshift, we have considered **five bins in Y_{500}** (Fig. 2). Within each bin we have selected five clusters randomly, giving preference to those that have been selected also for an on-going XMM large program (P.I.: M. Arnaud). We have limited our selection process to ACT and PSZ1 clusters but for two of them (selected from PSZ2), in order to reach the required number of five clusters in two of the boxes in the z - Y_{500} plane (cyan triangles in Figure 2). The systematic follow-up for confirmation and redshift determination has in fact been completed for PSZ1 but it is still on-going for PSZ2. So choosing clusters from the PSZ2 catalogue would bias our selection towards those for which the z information already exists. For the two largest Y_{500} boxes of the high redshift bin we have at present only 4 and 0 clusters. Therefore we have selected only 44 clusters for a total of about 210 hours. The 6 remaining clusters will be defined later, since in the coming years follow-ups will further populate the $z > 0.6$ region. We expect these 6 clusters to account for less than 10 hours of observing time. Then, in total, we will need 220 hours of on source observations. The selected clusters are given in Tab. 2 and 3. Finally, 50 hours will be dedicated to calibration. We have also reserved a total of 30 hours (10 % of the total) for possible loss of data due to bad weather, for example.

Complementary external data – The scientific output of the NIKA2 LP could be enriched by the use of high quality external data at other wavelengths. Other than the use of publicly available data, formal collaborations are expected to be established to collect extra proprietary data. At this regard, XMM data from a companion X-ray follow up of high redshift clusters will be used. With NIKA2 the cluster gas will be finally mapped in tSZ with a quality (in terms of sensitivity and angular resolution) comparable to X-ray, even for intermediate and high-redshift clusters. Then, the natural combination of these two direct observables of the intra-cluster hot gas (i.e., tSZ and X-ray measurements) will allow us to estimate the total masses (under the assumption of hydrostatic equilibrium) as well as a full physical characterization of the (radial) distribution of the cluster thermodynamic properties: not only pressure, but also temperature ($T_e(r) \propto P_e(r)/n_e(r)$) and entropy ($K(r) \propto P_e(r) n_e^{-5/3}$) which are essential to unveil cluster thermodynamic history. Indeed, the tSZ signal directly probes the gas pressure, while X-ray data deliver the gas density squared and temperature. The different dependencies of tSZ and X on the electron density will also provide a powerful probe of gas clumping, and an improved insight on the cluster tridimensional shape. Furthermore, optical follow-ups could be performed for a large number of the NIKA2 clusters using the GTC (Gran Telescopio Canarias) imaging and spectroscopy facilities. The combination of tSZ and X-ray data to optical/NIR observations of the cluster galaxies will further help to investigate the connection between galaxy properties (luminosity function, SFR, stellar mass) and those of the ICM, and thereby bring constraints on feedback mechanisms at play within clusters. Moreover, weak lensing measurements will provide complementary measurements of the dark matter distribution and total mass of the clusters, in a totally independent way, then affected by different systematics. Optical mass estimate are not based on the same assumptions.

NIKA2 will be able to observe simultaneously at two wavelengths, and this represents a great advantage for foreground source subtraction (Adam et al. 2015, Adam & NIKA collaboration in prep.). However PdBI, and its evolution into NOEMA (Northern Extended Millimetric Array project, 12 antennas with a diameter of 15 m, at 2550 m above the sea level), could be eventually used to obtain complementary information in this sense, requiring reasonable observing times.

Project management – For this project we have gathered a highly experienced team with a large expertise in sub millimetre observations, data reduction and tSZ science as well as complementary external observations. A project PI and two co-PIs will coordinate the different activities: data reduction (mainly former NIKA tSZ team), analysis and interpretation (former NIKA and Planck collaboration tSZ experts), and external ancillary data (XMM group for X-rays, LOFAR team for radio emission and GTC team for optical observations).

name	z	θ_{500} [arcmin]	$Y_{500} \times 10^{-4}$ [arcmin^2]	t_{obs} [hr]
ACTCLJ0241.2-0018	0.684	1.723	1.100	15.5
ACTCLJ0219.8+0022	0.537	2.169	1.700	21.4
ACTCLJ0240.0+0116	0.620	2.022	1.800	11.5
ACTCLJ0218.2-0041	0.672	2.005	2.200	7.6
ACTCLJ2050.5-0055	0.622	2.115	2.200	8.1
PSZ1 G073.22+67.57	0.609	2.311	3.276	6.2
PSZ1 G104.78+40.45	0.690	2.171	3.453	5.2
PSZ1 G086.93+53.18	0.675	2.255	3.961	4.1
PSZ1 G106.15+25.76	0.588	2.486	4.351	3.9
PSZ1 G094.54+51.01	0.539	2.656	4.757	5.1
PSZ1 G147.86+53.24	0.600	2.544	5.242	4.0
PSZ1 G070.91+49.26	0.604	2.561	5.544	3.6
PSZ1 G193.29-46.13	0.640	2.515	6.018	3.0
PSZ1 G183.92+42.99	0.561	2.735	6.281	3.1
PSZ1 G211.23+38.63	0.505	2.919	6.456	4.5
PSZ1 G201.50-27.34	0.538	2.905	7.616	3.2
PSZ1 G144.86+25.09	0.584	2.775	7.680	2.1
PSZ1 G046.13+30.75	0.569	2.818	7.710	2.1
PSZ1 G209.80+10.23	0.677	2.613	8.792	1.5
PSZ1 G102.86-31.07	0.591	2.837	8.988	2.3
PSZ1 G171.01+39.44	0.554	3.015	10.165	1.9
PSZ1 G228.21+75.20	0.545	3.043	10.201	1.9
PSZ1 G111.60-45.72	0.546	3.056	10.457	1.8
PSZ1 G155.25-68.42	0.566	3.019	10.951	1.6
PSZ2 G128.18-51.08	0.546	2.788	13.553	1.0

Table 2: $0.5 \leq z < 0.7$ selected sample: 25 clusters.

Data policy – The project data and products will be made publicly available by the NIKA2 collaboration in a dedicated database, following the standard IRAM rules.

References

Adam, R., Adane, A., Ade, P., et al. 2014a, Proceedings of the 49th rencontres de Moriond : Cosmology, La Thuile (Italy), 22-29 March 2014

Adam, R., Comis, B., Macías-Pérez, J.-F., et al. 2015, A&A, 576, A12

Adam, R., Comis, B., Macías-Pérez, J. F., et al. 2014b, A&A, 569, A66

Aghanim, N., Hurier, G., Diego, J.-M., et al. 2014, ArXiv e-prints

Arnaud, M., Pratt, G. W., Piffaretti, R., et al. 2010, A&A, 517, A92

Bleem, L. E., Stalder, B., de Haan, T., et al. 2014, ArXiv e-prints

Böhringer, H., Schuecker, P., Pratt, G. W., et al. 2007, A&A, 469, 363

Carlstrom, J. E., Holder, G. P., & Reese, E. D. 2002, ARA&A, 40, 643

Czakon, N. G., Sayers, J., Mantz, A., et al. 2014, ArXiv e-prints

Hasselfield, M., Hilton, M., Marriage, T. A., et al. 2013, J. Cosmology Astropart. Phys., 7, 8

Korngut, P. M., Dicker, S. R., Reese, E. D., et al. 2011, ApJ, 734, 10

Mroczkowski, T., Dicker, S., Sayers, J., et al. 2012, ApJ, 761, 47

Plagge, T., Benson, B. A., Ade, P. A. R., et al. 2010, ApJ, 716, 1118

Planck Collaboration, Ade, P. A. R., Aghanim, N., et al. 2014, A&A, 571, A29

Planck Collaboration, Ade, P. A. R., Aghanim, N., et al. 2013, A&A, 550, A131

Planck Collaboration, Ade, P. A. R., Aghanim, N., et al. 2015a, ArXiv e-prints

Planck Collaboration, Ade, P. A. R., Aghanim, N., et al. 2015b, ArXiv e-prints

Planck Collaboration, Aghanim, N., Arnaud, M., et al. 2015c, ArXiv e-prints

name	z	θ_{500} [arcmin]	$Y_{500} \times 10^{-4}$ [arcmin^2]	t_{obs} [hr]
ACTCLJ0228.5+0030	0.720	1.641	1.000	17.7
ACTCLJ0250.1+0008	0.780	1.618	1.200	12.0
ACTCLJ0018.2-0022	0.750	1.739	1.500	8.4
ACTCLJ0058.0+0030	0.760	1.742	1.500	8.5
ACTCLJ0215.4+0030	0.865	1.648	1.800	5.5
ACTCLJ0059.1-0049	0.786	2.002	3.500	3.0
ACTCLJ0022.2-0036	0.805	2.008	3.800	2.5
PSZ1 G089.04+55.07	0.702	2.215	4.071	3.8
PSZ1 G226.65+28.43	0.724	2.190	4.209	3.5
PSZ1 G084.04+58.75	0.731	2.213	4.586	3.0
PSZ1 G065.13+57.53	0.720	2.295	5.322	2.3
PSZ1 G091.82+26.11	0.822	2.192	6.306	1.6
PSZ1 G048.09+27.18	0.736	2.355	6.553	1.6
PSZ1 G224.73+33.65	0.768	2.303	6.647	1.5
PSZ1 G141.73+14.22	0.830	2.209	6.789	1.4
PSZ1 G183.26+12.25	0.850	2.226	7.637	1.1
PSZ1 G080.66-57.87	0.705	2.518	8.182	1.6
PSZ2 G160.83+81.66	0.888	1.907	9.043	1.0
PSZ1 G138.60-10.85	0.702	2.618	9.669	1.2

Table 3: $0.7 \leq z < 0.9$ selected sample.

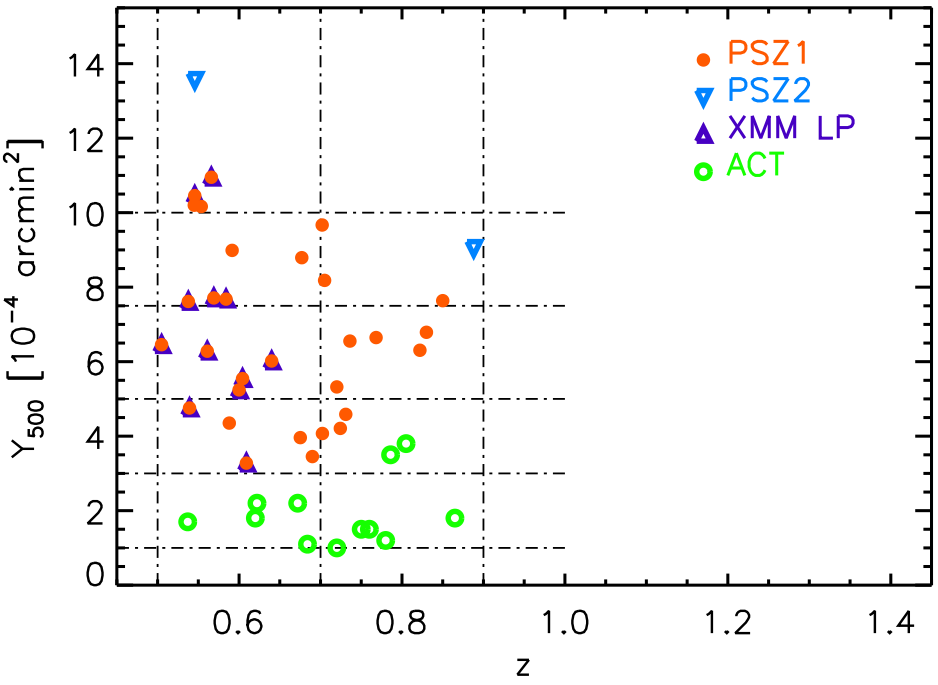

Figure 2: Selected sample of 44 clusters extracted from the Planck and ACT (equatorial) tSZ-selected cluster catalogues, selected from those fulfilling our redshift (> 0.5) and observability (dec > -11) criteria. The selected objects are shown in the Y_{500} - z plane.

Reichardt, C. L., Stalder, B., Bleem, L. E., et al. 2013, ApJ, 763, 127
Sayers, J., Czakon, N. G., Mantz, A., et al. 2013, ApJ, 768, 177
Sayers, J., Golwala, S. R., Ameglio, S., & Pierpaoli, E. 2011, ApJ, 728, 39
Young, A. H., Mroczkowski, T., Romero, C., et al. 2014, ArXiv e-prints